White-Light Emissive Silver-Exchanged Nanoporous NaP1 Zeolites

José Adán Moreno-Torres, Aurore Lecharlier, Fabricio Espejel-Ayala, Johan Hofkens, Eduard Fron, Maarten B J Roeffaers, Eduardo Coutino-Gonzalez, Rafael Ramírez-Bon

ACS APPLIED NANO MATERIALS

www.acsanm.org

Article

White-Light Emissive Silver-Exchanged Nanoporous NaP1 Zeolites

José Adán Moreno-Torres, Aurore Lecharlier, Fabricio Espejel-Ayala, Johan Hofkens, Eduard Fron, Maarten B. J. Roeffaers, Eduardo Coutino-Gonzalez,* and Rafael Ramírez-Bon*

Cite This: *ACS Appl. Nano Mater.* 2024, 7, 11965−11972

Read Online

ACCESS | Metrics & More | Article Recommendations | Supporting Information

ABSTRACT: Silver nanoclusters (Ag-NCs) encapsulated into zeolite scaffolds, a class of photostable luminescent nanomaterials, have aroused great interest due to their attractive photoluminescence (PL) properties and promising applications as alternative phosphors for light-emitting devices. However, current research predominantly features single-color emitters in luminescent Ag-exchanged zeolites. Herein, the synthesis and characterization of white-light emissive Ag-exchanged NaP1 zeolites obtained from natural clinoptilolite through hydrothermal processes are described. Samples were subjected to X-ray diffraction (XRD), scanning electron microscopy (SEM), X-ray photoelectron spectroscopy (XPS), steady-state PL spectroscopy, and fluorescence microscopy analysis. Optically and chemically pure NaP1 zeolites were obtained from nonconventional precursors and subsequently exchanged with Ag loadings (12.5, 25, 33, 50, and 66 wt %), resulting in luminescent samples after a thermal activation at 450 °C with quantum efficiencies of up to 6.2% and a broad emission band (full width at half-maximum = 31250 cm^{-1}) when excited at 380 nm. The strategy to obtain white-light emissive materials presented in this study opens alternative avenues for the development of sustainable phosphors, decreasing the burden of nonrenewable resources.

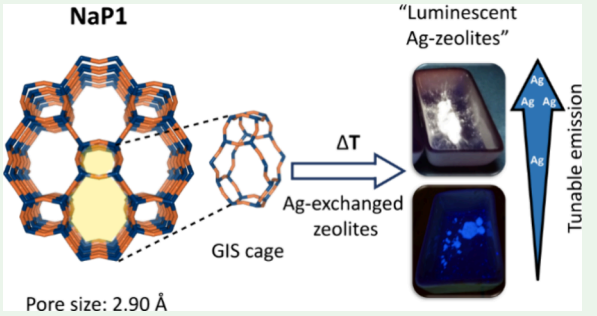

KEYWORDS: *silver nanoclusters, small-pore NaP1 zeolites, photoluminescence, NUV-LED phosphors, white-emitting phosphors*

INTRODUCTION

Luminescent silver nanoclusters (Ag-NCs) encapsulated within zeolites can have outstanding emissive properties including large Stokes shifts, high external quantum efficiencies (EQEs), and exceptional photostability, among others.[1,2] These optical properties depend not only on the zeolite framework, the Ag loading, and the presence of specific counterbalancing ions but also on the hydration conditions. This remarkable versatility allows for a tunable optical emission that spans nearly the entire visible range and can achieve EQEs approaching unity.[3−6] These features render zeolite-stabilized Ag-NCs as promising phosphors for LEDs and as active layers in electroluminescent devices.[7] Within this scenario, a variety of Ag-NCs formed inside different zeolite topologies have been reported, among the most widely studied are Linde type A (LTA), faujasite (FAU), and sodalite (SOD) zeolites displaying visible emission ranging from blue to red.[3−5,8−12] However, white-light-emitting single-phase phosphors spanning the entire visible range from 400 to 700 nm are more desirable for manufacturing white-light-emitting diodes (WLEDs). These devices offer several advantages, such as higher efficiency compared to incandescent lamps, do not contain toxic mercury like fluorescent lamps, and provide higher color stability and reproducibility compared to multicomponent phosphor-based WLED (e.g., blue, green, and red with near-ultraviolet (NUV) chips and yellow with blue chips) as well as lower production costs. These attributes position them as a promising and sustainable choice for the future of lighting technology.[7]

To date, several studies have reported the broad white-light emission from Ag-NCs-zeolite composites for application as phosphor in WLEDs.[11,13−16] Previously, Yao et al.[13] reported an Ag-exchanged FAU-Y zeolite with tunable emission (from green to cyan) calcined at different temperatures and obtained a single-component white-light phosphor at elevated temperatures (950 °C). Moreover, SOD zeolite has been employed as a confinement scaffold to stabilize white-light-emissive Ag-NCs-based composites by heating the SOD zeolite codoped with Ag^+, Eu^{3+}, and Zn^{2+} at 800 °C[15] or by controlling the extraframework cations (Li^+, Na^+, K^+, Cs^+, Mg^{2+}, and Ca^{2+}), heat treatment temperature, and Ag loading.[11] Recently, Baekelant and collaborators succeeded in obtaining highly luminescent white-light-emissive Ag zeolites. To achieve this, a combination of chalcogenide species (specifically, sulfur anions) and Ag-NCs was stabilized within a SOD zeolite matrix.[14]

Received: March 15, 2024
Revised: May 1, 2024
Accepted: May 3, 2024
Published: May 13, 2024

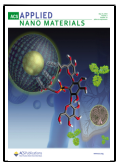

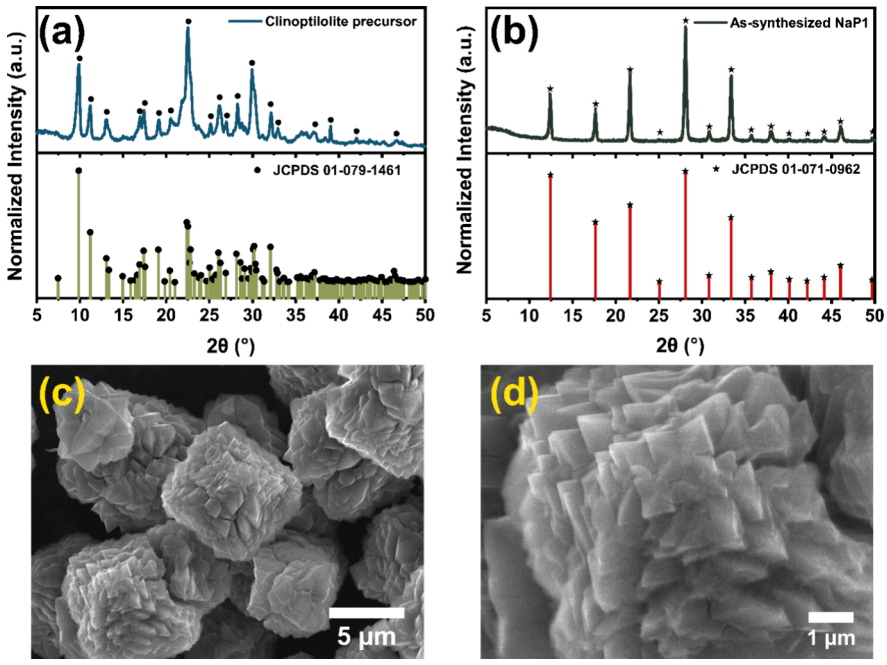

Figure 1. (a, b) XRD patterns of the powdered natural clinoptilolite precursor after calcination at 450 °C and zeolite product (obtained from 1 M NaOH, 24 h−90 °C of HT) compared to clinoptilolite and NaP1 zeolite references, respectively. (c, d) SEM micrographs of the obtained NaP1 zeolite at different magnifications.

Nonetheless, the quest for single-phase white-light-emitting Ag-zeolite phosphors has prompted the exploration of other zeolite topologies, in particular small-pore size zeolites (i.e., eight-membered ring, 8-MR), where the stabilization of ultrasmall noble metal nanoclusters (NCs) has been demonstrated.[17−19] Recently, Li et al.[16] achieved Ag-NCs zeolite composites using small-pore analcime (ANA) as hosts and terephthalic acid to avoid the formation of Ag nanoparticles on the zeolite surface; such samples displayed adjustable emission ranging from orange through yellow to white, showing the great potential of small-pore zeolites to tune the optical properties of the stabilized metal NCs.

Herein, we report the production of a white-light-emissive Ag-zeolite phosphor using small-pore NaP1 zeolites after a cation exchange procedure followed by thermal treatment at 450 °C. NaP1 zeolites with gismondine (GIS) structure possess an open [tetrahedral] framework due to the high flexibility of the Si−Al linkage. This flexibility allows both expansion and contraction of the framework along with the dynamics of out-of-framework cation movement, being an intrinsic property of zeolites. This behavior originates from the elasticity of the Si−O and Al−O bonds, as well as the deformation of the Si−O−Al and Si−O−Si angles, in response to external factors such as guest hosts, composition, and variations in temperature or pressure.[20,21] The small-pore NaP1 zeolites used in our study were synthesized from natural clinoptilolite zeolites, offering an alternative source of Si and Al, through alkaline hydrothermal treatments (HT), and subsequently employed to confine luminescent Ag-NCs, making them high-value-added synthetic zeolites produced from low-cost raw materials. Moreover, we observed that by varying the Ag content in Ag-NaP1 zeolite composites a tunable emission from violet, blue to white was achieved, where the tunability of their emission properties was tentatively ascribed to the formation of luminescent Ag_3 and Ag_4^{2+} NCs within the cavities of the as-synthesized NaP1 zeolites.[4,5,8] As a result, a white-light-emitting phosphor with CIE color coordinates of (0.30, 0.32) under NUV excitation (380 nm) was obtained. To the best of our knowledge, this report addresses the first rationally designed study of Ag-exchanged NaP1 zeolites (obtained through sustainable routes) with tunable emission (from violet to blue and white).

EXPERIMENTS AND METHODS

Generation of Optically Pure NaP1 Zeolites Starting from Natural Zeolite Clinoptilolite. NaP1 zeolites were synthesized via alkaline dissolution of the clinoptilolite, followed by a hydrothermal treatment as described elsewhere.[22] It is worth noting that natural clinoptilolite contains several extraframework cations, including Na^+, K^+, Ca^{2+}, and Mg^{2+}. Additionally, traces of iron (Fe^{3+}) were detected, presumably replacing Si atoms in the tetrahedral sites of the zeolite structure.[23] Among these cations, K^+ was found to be the most concentrated, while Fe^{3+} was present at trace levels (Figure S1). Interestingly, the presence of Fe^{3+} contributed to the distinct coloration of the powder, appearing light beige before calcination and transforming into a strong beige hue after calcination (Figure S2).[24,25] Moreover, SEM analysis on the clinoptilolite precursor revealed crystals with irregular morphology (Figure S3).

Silver Exchange Procedure. Ag-exchanged NaP1 zeolites were prepared using the procedure described elsewhere.[3] Samples with different Ag loadings (12.5, 25, 33, 50, and 66 wt % of $AgNO_3$ with respect to the zeolite; see the Supporting Information) were prepared to investigate the influence of Ag loading on the photoluminescence (PL) properties. Samples were denoted as NaP1-Ag_x, where x represents the wt % of $AgNO_3$ precursor utilized in the cation exchange procedure (for instance, NaP1-$Ag_{12.5}$ corresponds to the as-synthesized NaP1 zeolite exchanged with 12.5 wt % of $AgNO_3$).

X-ray Diffraction (XRD) Analysis. XRD data were acquired utilizing a D8 Advance Bruker diffractometer with Cu $K\alpha_1$ radiation (1.541 Å) in the range of 2θ = 10°−60° using a scanning speed of 0.02°/s. Subsequently, the XRD patterns underwent indexing employing the recognized standard diffraction patterns for clinoptilolite and NaP1 zeolite, as outlined by the International Zeolite Association (IZA).[26]

https://doi.org/10.1021/acsanm.4c01565
ACS Appl. Nano Mater. 2024, 7, 11965−11972

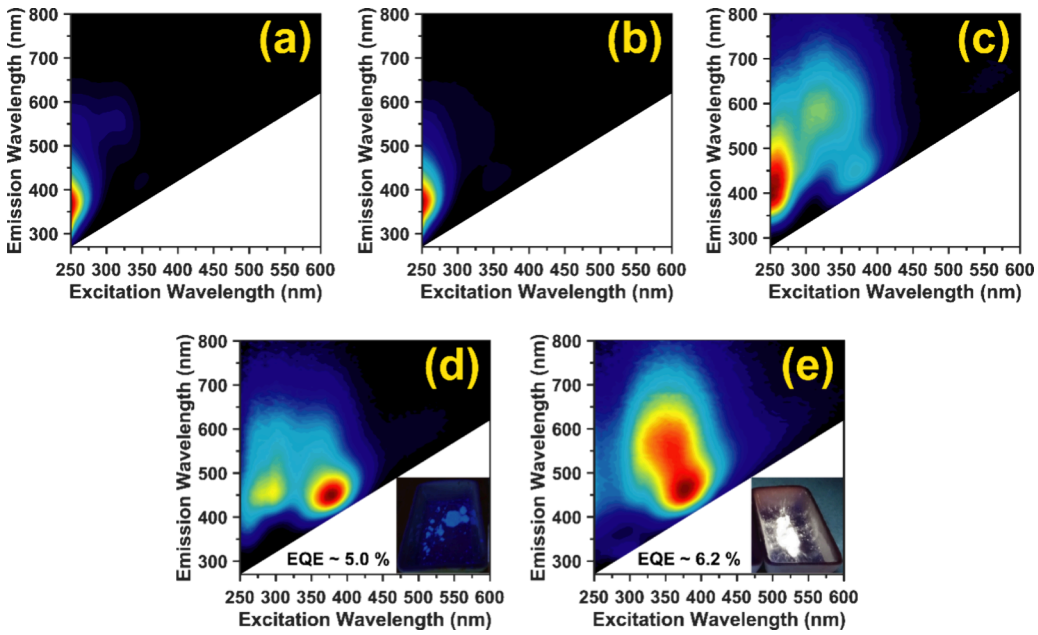

Figure 2. 2D excitation−emission plots of Ag-exchanged NaP1 zeolites synthesized from clinoptilolite with different Ag loadings: (a) NaP1-$Ag_{12.5}$, (b) NaP1-Ag_{25}, (c) NaP1-Ag_{33}, (d) NaP1-Ag_{50}, and (e) NaP1-Ag_{66}. The insets in (d) and (e) show pictures of the samples under UV illumination at 365 nm.

Scanning Electron Microscopy (SEM) and Energy-Dispersive Spectroscopy (EDS). SEM and EDS images were obtained on a JEOL 6500LV device equipped with an X Flash 6110 Bruker detector.

Thermogravimetric Analysis (TGA). TGA analysis was conducted on a Q500 TGA instrument from TA Instruments. The zeolite sample, weighing 10−30 mg, was placed in a platinum holder and heated from room temperature to 600 °C using a temperature ramp of 3 °C/min, under a continuous N_2 flow of 90 mL/min.

X-ray Photoelectron Spectroscopy (XPS). XPS spectra were obtained by using a Thermo Scientific K-Alpha XPS system. The Al Kα source emitted X-ray radiation at 1486.7 eV, focused onto a 200 × 200 μm^2 spot with a power density of 66 W/m^2.

Steady-State Optical Properties. Steady-state PL properties, including two-dimensional (2D) excitation−emission plots and EQEs, were recorded by using an Edinburgh FLS980 fluorometer. EQE was measured using an integrating sphere (Labsphere) connected to the fluorometer via optical fibers, using barium sulfate as a total dispersion reference. The emission profiles obtained were deconvoluted with Gaussian-shaped peaks, using the multipeak fitting in the Origin Pro 2018 software. Confocal fluorescence microscopy (Confocal Olympus FluoView FV-1000 + fully motorized Olympus IX81 inverted microscope) was used to analyze the luminescence of individual NaP1-Ag_x crystals and the heterogeneity in the emitted color and intensity among individual crystals.

Fluorescence Microscopy. An Olympus FluoView FV-500 microscope was used as a wide-field epifluorescence microscope. A mercury light source is used for the illumination of the sample. The range of the excitation spectra is selected using a band-pass filter. The band-pass filter used passes light from 310 to 390 nm, with a maximum at around 350 nm. A Canon EOS 5D Mark II camera was used to capture all pictures of the illuminated samples positioned in place of the eyepiece lens.

RESULTS AND DISCUSSION

Synthesis and Characterization of Single-Phase NaP1 Zeolites Using Clinoptilolite as Precursor. Figures 1a and 1b display the diffractograms of natural clinoptilolite and the as-synthesized NaP1 zeolite, respectively, as confirmed by the reference files JCPDS No. 01-79-1461 and JCPDS No. 01-71-0962.[26−28] It is worth noting that the XRD pattern of the as-synthesized NaP1 zeolite shows neither the appearance of characteristic diffraction peaks associated with the clinoptilolite precursor nor the presence of other zeolitic phases, suggesting the effective synthesis of a single-phase NaP1 zeolite suitable to host−metal NCs.[4,5]

SEM analysis (Figures 1c and 1d) reveals the highly intergrown of cuboctahedron-shaped crystals, similar to those observed for NaP1 zeolites in previous reports.[25,29,30] EDS (Figure S1) measurements confirm that besides Si, Al, and O as the main elements, the natural clinoptilolite precursor also contains extraframework cations such as K^+, Na^+, Mg^{2+}, Ca^{2+}, and Fe^{3+} in lower concentrations. Similarly, the EDS and XPS data show that Si, Al, O, and Na are the main components in the as-synthesized NaP1 (Figures S5 and S6) and Na^+ is the main counterbalancing cation in the zeolite structure, whereas K^+ and Ca^{2+} were present only in trace amounts and no Fe^{3+} could be detected, suggesting a high chemical purity of the as-synthesized zeolite. The average Si/Al ratios of the clinoptilolite precursor and the as-synthesized NaP1 zeolite are 4.8 and 1.7, respectively, matching very well with Si/Al ratios of previously reported for NaP zeolites (1.1−2.5).[31] The XPS analysis further supports this, determining that the Si/Al ratio in the NaP1 framework accounts for 1.58 (see also Figure S6).

Diffuse reflectance spectroscopy (DRS) analysis was also performed to investigate the optical purity of the zeolite obtained. The DRS spectrum of the as-synthesized NaP1 zeolite shows higher absorption in the range λ < 350 nm compared to commercial zeolites (LTA, FAU), as depicted in Figure S7. Zeolites exhibit absorption bands in the short-wavelength range attributed to charge transfer $O^{2-} \rightarrow Al^{3+}$, involving aluminum atoms at specific sites (surfaces, corners, and defects).[32,33] However, no additional bands in the range λ > 350 nm are observed discarding the predominant presence of extra cationic impurities such as K^+ and Ca^{2+}.[33] Additionally, TGA was performed to assess the water content of the as-synthesized NaP1 zeolite. TGA analysis (Figure S8) revealed a

https://doi.org/10.1021/acsanm.4c01565
ACS Appl. Nano Mater. 2024, 7, 11965−11972

total weight loss of approximately 13.5 wt % by 500 °C, occurring in two stages. The first stage (62.5−250 °C) corresponds to the release of water molecules from the micropores, with peak loss at 100 °C. The second stage (250−500 °C) involves the decomposition and elimination of hydroxyl groups, peaking at around 325 °C.[34,35]

Luminescent Properties of Ag-Exchanged NaP1 Zeolites. To study the PL properties of NaP1-Ag_x samples with varying Ag loadings (x = 12.5, 25, 33, 50, and 66 wt %), 2D excitation−emission PL plots were recorded. Figure S9 provides a summary of the different emission and excitation bands in relation to the Ag loadings. Figures 2a and 2b show the 2D excitation−emission plots of NaP1-$Ag_{12.5}$ and NaP1-Ag_{25} samples, where a weak emission in the UV region with a maximum between 365−370 nm when excited at around 250 nm is present. In contrast, the NaP1-Ag_{33} sample displays new broad visible light emission (Figure 2c). The visible emission is most intense in the violet and has a long tail into the green-yellow when excited in the deep-UV. Additionally, a new PL band centered at around 450 nm when exited at 370 nm emerged. The violet emission was also reported by Aono et al.[19] for Ag-exchanged NaP1-type zeolite after mild heat treatment (between 100−200 °C). Further, they investigated the impact of heat treatment on the luminescent characteristics of the Ag-zeolite composites, resulting in an emission of 390 nm (violet color) for samples subjected to 800 °C heating. However, it is essential to highlight that in their study the NaP1 phase began to diminish and eventually disappear after reaching temperatures above 400 °C. Unlike this report, our samples were treated at 450 °C to obtain highly luminescent materials (Figures 2d,e, insets). Importantly, the cation exchange and heat treatment processes did not affect the well-defined structure of the as-synthesized NaP1 zeolite (Si/Al = 1.7),[36] in agreement with the X-ray diffraction patterns (Figure S10). The structural integrity of the sample demonstrated consistency as compared to that of the non-calcined sample, previously observed.[36]

Figures 2d and 2e (insets) show blue-white to bright-white emission of NaP1-Ag_{50} and NaP1-Ag_{66} samples under near-UV excitation (365 nm) with EQE values of 5.0 and 6.2%, respectively. For the NaP1-Ag_{50} sample, a red-shift in the maximum of the emission (from 400 to 453 nm) and excitation bands (from 255 to 290 nm and 370 to 380 nm) with respect to the NaP1-Ag_{33} sample is observed (Figure S9). Instead, in the NaP1-Ag_{66} sample, a luminescent band centered at about 465 nm, accompanied by a clear shoulder at around 600 nm, is observed. Interestingly, the excitation band at 290 nm decreases, while the excitation band at 380 nm remains the same. The maxima of all PL bands and EQEs of the Ag-loaded NaP1 zeolites are summarized in Table 1.

The low Ag loadings (12.5 and 25 wt %) probably did not lead to significant Ag-NCs formation inside the zeolite framework due to the shortage of interactions between the Ag atoms during the thermal activation.[37] In the NaP1-Ag_{33} sample the emergence of new excitation bands (at 370 nm) can be tentatively ascribed to the formation of different luminescent Ag species at specific sites inside the NaP1 structure.[38] Furthermore, there is still hydration water present in small amounts during calcination of zeolite at 450 °C (Figure S8), which is necessary for the thermal autoreduction process leading to the formation of Ag-NCs.[3] The red-shift observed in the excitation bands, from 255 to 290 nm and 370 to 380 nm in the NaP1-Ag_{50} sample, could be attributed to

Table 1. Summary of the Ag Loaded NaP1 Zeolites at Various Ag Ratios with Their Corresponding Luminescence Bands and EQEs

exchanged conditions		PL features of the Ag-exchanged zeolite		
zeolite	Ag-exchange ratio (wt %)	Em_{max} (nm)	Exc_{max} (nm)	EQE (%)[a]
NaP1 (1 M NaOH, 24 h−90 °C of HT)	12.5	365	250	
	25	370	250	
	33	400	255, 370	
	50	453	290, 380	5.0
	66	465	380	6.2

[a]The measurement error on the absolute EQE is 2%.

alterations in the interaction level of Ag cations with the framework oxygen and their arrangement within the zeolite scaffold.[39]

Further spectral analysis of NaP1-Ag_{50} and NaP1-Ag_{66} samples by fitting the emission spectra with multiple Gaussian peaks (Figure 3) revealed the presence of two main PL bands

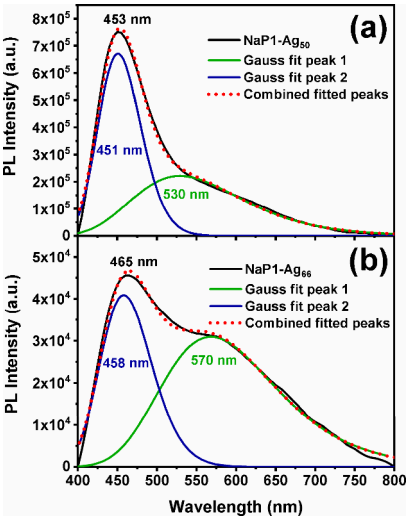

Figure 3. Spectral deconvolution of the emission profiles obtained under excitation at 380 nm of the (a) NaP1-Ag_{50} and (b) NaP1-Ag_{66} samples.

for the two Ag-NCs-zeolite composites, an emission maximum at 451 nm and a second emission band at 530 nm, upon excitation at 380 nm, for the NaP1-Ag_{50} sample; whereas for the NaP1-Ag_{66} sample, a blue emission band centered at 458 nm and a green broadband centered at approximately 570 nm, under excitation at 380 nm, are visible. A similar blue emission behavior was previously described in partially hydrated Ag-exchanged Li-LTA zeolites at low Ag loadings, whose emission was assigned to low nuclearity Ag-NCs (Ag_3) characterized by X-ray absorption fine structure (EXAFS) analysis.[8] Note that the emission band between 450−465 nm excited at 380 nm remains unaltered; hence, this suggests the confinement of a small stable Ag_3 blue-emitting NC into the small voids of the as-synthesized NaP1 zeolite. The spectral broadening of the emission band at 570 nm (excitation at 380 nm) indicates the existence of an electron−phonon interaction between the confined Ag-NC species and the zeolite structure.[40] Besides,

https://doi.org/10.1021/acsanm.4c01565
ACS Appl. Nano Mater. 2024, 7, 11965−11972

the emission bands red-shifted and broadened from 530 to 570 nm by increasing Ag concentration. This phenomenon could be explained by the increased size of the NCs-emitting species in the excited state compared with the ground state. Consequently, the separation between the emission peaks can be attributed to the electron−phonon coupling effect related to changes in the Ag−Ag and Ag−O bond distances.[41] A similar broadband emission in the yellow-greenish region has been observed in Ag-exchanged LTA-type zeolites with low to intermediate Ag loadings; such emission has been associated with an Ag_4^{2+} type NC.[4,5] Therefore, the emission bands at 530 and 570 nm are tentatively assigned to the formation of Ag_4^{2+} NCs.

To gain insight into the lifetimes of the Ag-NCs species present in the NaP1-Ag_{66} sample, we conducted time-resolved luminescence measurements on a scale of nanoseconds to milliseconds within a 1 ms time window. Luminescence decays were determined using an excitation wavelength of 365 nm and two detection wavelengths (450 and 580 nm) selected according to the spectral deconvolution of the emission profile of the NaP1-Ag_{66} sample (Figure 3b). The fit analysis at 450 nm detection (Figure S11a) reveals, besides a very fast decaying component, two components of 0.52 and 65 μs. Additionally, three components (0.92, 24, and 260 μs) were observed under 580 nm detection (Figure S11b), suggesting the presence of different emitting species under different confinement environments, as previously reported.[8,41]

The variations in emission that occur with an increasing amount of Ag suggest the coexistence of different types of Ag-NCs within the zeolite matrix. It is noteworthy that the highest loading used in this study (66 wt %) closely approaches the theoretical total exchange capacity of the as-prepared zeolite (68 wt %, as described in the Supporting Information). Therefore, we foresee that a further increase in Ag loading, as the theoretical full exchanged capacity has been reached, would have no impact on the cation exchange process and in the formation of Ag-NCs.[42]

White-Light Emission of Ag-Exchanged NaP1 Zeolites. Fluorescence microscopy was employed to observe whether different luminescent species are present homogeneously in several NaP1-Ag_{66} crystals. In each area, the luminescence in three wavelength regions (435−535, 535−635, and 635−755 nm) was recorded corresponding to the working range of three PMT detectors preceded by dichroic mirrors, as depicted in Figures 4a−c. Moreover, the PL of seven labeled areas was analyzed in detail (Figure 4d), collecting the photoluminescent data for each wavelength scan (emission spectra from ∼420 to 700 nm in 5 nm steps, at 405 nm excitation). Where regions 1−6 correspond to emitting zeolite crystals, and region 7 was taken as a reference to distinguish between photoluminescent crystals and the background. The analysis of the first area highlights that, collectively, all crystals emit light spanning almost the entire visible range (435−755 nm), explaining the apparent white homogeneous luminescence of the sample at bulk level. Figure 4e displays the emission spectra of all NaP1-Ag_{66} regions analyzed in the first selected area, wherein a broad spectral region was observed from 420 to 720 nm, confirming white-emitting Ag zeolites except in regions 2, 4, and 7, where region 7 proves that there was no contribution from background emission. It is worth mentioning that there are no significant groups of crystals emitting at different wavelengths. Consequently, this homogeneous emission could result from a uniform distribution of Ag-NCs species in the zeolite crystal population. Nevertheless, few individual crystals are spotted emitting at a specific PL emission wavelength. The emission spectrum of region 2 is blue-shifted by 55 nm, and the emission spectrum of region 4 is slightly red-shifted by 30 nm than the rest, as observed in Figure 4e. These differences in crystal emission are confirmed by wide-field fluorescence microscopy (Figure S12).

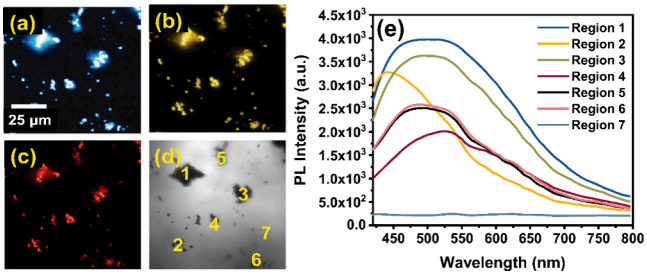

Figure 4. Fluorescence images of the NaP1-Ag_{66} sample corresponding to the following detection channels: (a) 435−535 nm, (b) 535−635 nm, and (c) 635−755 nm. (d) Transmission of individual crystals and their respective locations. (e) Emission scans of NaP1-Ag_{66} crystals excited at 405 nm measured on a confocal fluorescence microscope. Region 7 corresponds to the nonemitting background.

In Figure S13, two additional wide-field fluorescence images of a second sample area are displayed, also exhibiting a blue-emitting crystal and slightly orange-reddish-emitting crystals surrounded by a multitude of white-light-emitting crystals, which is in good agreement with the PL observations. This could be due to certain reasons. One possibility is the difference in the degree of Ag exchanged between individual crystals, and consequently, the Ag-NCs species development in each crystal may differ, as reported by Plessers et al.[43] where changes in the coloration of single crystal silica supported Ag nanoparticles due to local Ag gradients were observed. Variations in the Si/Al ratio (as previously observed in the EDS and XPS results, Figures S5 and S6, respectively) of individual crystals and their remaining co-cations may also play a major role since the Ag-NCs could experience a different electronic environment in each single zeolite crystal. For instance, Fleury et al.[44] reported that the structure and distribution of aluminum in mordenite zeolite vary significantly depending on the extent of dealumination. Concerning the co-cations, it is reasonable to consider the possibility that they affect the clustering of the exchanged Ag^+ ions. Yao et al.[11] recently reported the role of co-cations (Li^+, Na^+, K^+, Cs^+, Mg^{2+}, and Ca^{2+}) in the optical properties of Ag-NCs stabilized in SOD zeolites. Their investigation revealed a remarkable capacity to adjust the luminescent emissions of Ag-NCs from blue, yellow, and orange to a warm white color; they assigned this behavior to the nature of the cations, inducing a lattice shrinkage of the framework of the SOD zeolites. As previously observed by the XPS results (Figure S6), trace amounts of K^+ and Ca^{2+} were found in the as-synthesized NaP1 zeolite. Hence, these irregularities in the emission of certain individual grains could be ascribed to variations in counterbalancing cations such as Na^+, K^+, and Ca^{2+} present in the Ag-exchanged NaP1 zeolites. To minimize these heterogeneities, it is feasible to adjust the synthesis conditions to promote more uniform nucleation and growth. Additionally, an acid treatment of the initial clinoptilolite could improve the purity of the starting material decreasing the metal impurities, resulting in a host

https://doi.org/10.1021/acsanm.4c01565
ACS Appl. Nano Mater. 2024, 7, 11965−11972

with higher chemical and optical purity. This direct improvement in purity, together with the fine-tuning of the activation step through reduction−oxidation cycles, could boost the EQE performance of the white-emitting materials.[42]

Additionally, XPS analysis was performed to elucidate the electronic state of the Ag species present in the NaP1-Ag_{66} sample (Figure S14). Signals associated with O, Si, and Al elements of the XPS survey spectrum are observed. However, the Na signal decreases, and the appearance of a new intense signal is detected, attributed to Ag species, proving that the Ag^+ ions were introduced into the zeolite. No evident changes in the peak positions of the signals in the O 1s, Si 2p, Al 2p, and Na 1s regions are observed in the high-resolution spectra. Whereas for the Ag 3d region, two main peaks corresponding to binding energy of Ag $3d_{5/2}$ and Ag $3d_{3/2}$ are spotted. The binding energy of $Ag_{5/2}$ displays an intense peak centered at 368.58 eV, which is higher than that of Ag metal (368.20 eV),[4] potentially ascribed to subnanometer Ag-NCs within the zeolite cavities.[4,7]

The bright-white-light emission of the NaP1-Ag_{66} sample indicates that it originates from mixing of the emission of two types of Ag-NCs present within the channels of the as-synthesized NaP1 zeolite. These findings show that the zeolite framework plays a major role in tuning its opto-structural properties since the nature of the NCs is determined by the topology of the framework, the framework charge, and interaction with other extraframework cations.[7] As mentioned above, the framework of NaP1 zeolite shows exceptional flexibility without framework degradation.[27] In this regard, Choi et al.[45] recently reported NaP-type zeolites with Si/Al ratios of 1.5, 3.0, and 4.7, in which Na^+ ions occupied two almost identical sites within the zeolite structure for all samples in their hydrated form. The first site for the Na^+ ion is centered within the 8-MR windows and is octahedrally coordinated by six water molecules. The second site, located within the 8-MRs, is slightly off-center and within the interaction distance with the oxygen atoms of the framework. Upon dehydration, the framework is distorted, and Na^+ ions move from the windows of the 8-MRs closer to the framework into the pockets of the dcc units, resulting in substantial compression forces, showing a preference for the channel crossing, as illustrated in the scheme depicted in Figure S15. That could explain the appearance of two types of small Ag-NCs, where the Ag^+ ion replaces the specific Na^+ ion sites. Upon heat treatment of the samples, the structure is distorted and compressed such that the NCs are positioned within the two channels; the Ag_3 and Ag_4^{2+} species could occupy the smallest (dcc) and largest channel (8-MR), respectively (Figure S15). Previously, Yao and collaborators[13] reported white-light emission in Ag-exchanged FAU-Y zeolites heat-treated at 950 °C, where the collapsing of the zeolite framework was observed, associating the white emission to the interaction of Ag^+−Ag^0 and Ag^+−Ag^+ species formed during the destruction of the zeolite framework. In contrast, in our samples, the use of elevated temperatures was not necessary; this way our approach could be an affordable alternative in the generation of white-light emission in Ag-exchanged zeolites using sustainable small-pore zeolites.

Assessment of Ag-Exchanged NaP1 Zeolites as White-Emissive Phosphors for Lighting Devices. The emission spectra of the NaP1-Ag_x samples were converted to the Commission Internationale de l'Eclairage (CIE) 1931 chromaticity diagram (Figure 5) to find the lighting color area

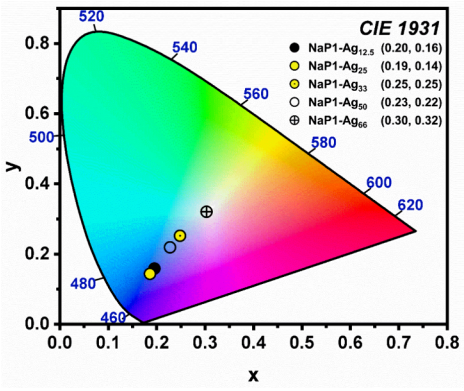

Figure 5. CIE-1931 chromaticity coordinates of NaP1-Ag_x samples. The CIE coordinates for NaP1-$Ag_{12.5,25,33}$ samples were obtained from their emission spectra upon excitation at 250 nm, while for NaP1-$Ag_{50,66}$ samples were obtained under 380 nm excitation.

of each Ag-exchanged sample. The corresponding CIE (x, y) chromaticity coordinates were determined as (0.20, 0.16), (0.19, 0.14), and (0.25, 0.25) when excited at 250 nm for NaP1-$Ag_{12.5}$, NaP1-Ag_{25}, and NaP1-Ag_{33} samples, respectively, whereas for NaP1-Ag_{50} and NaP1-Ag_{66} samples, their CIE coordinates were (0.23, 0.22) and (0.30, 0.32), respectively, at 380 nm excitation. The above indicates a tunable emission color of the samples ranging from violet to white as the Ag concentration in the zeolite structure increases. Importantly, the obtained NaP1-Ag_{66} sample has the CIE color coordinates of (0.30, 0.32) and an appropriate CCT of 7189 K, which are very close to the CIE coordinates (0.33, 0.33) of the ideal pure-white-light emission.[14] In addition, the emission spectra of NaP1-Ag_{50} and NaP1-Ag_{66} samples (Figure S16a) under a 290 nm excitation wavelength were used to obtain their CIE coordinates. Significant changes in the CIE coordinates (0.27, 0.29) and (0.33, 0.37) were observed for the NaP1-Ag_{50} and NaP1-Ag_{66} samples (Figure S16b), respectively. These results indicate that a wavelength of 380 nm is optimal for using these materials as phosphors in NUV-LED devices.

The excellent performance of phosphors against temperature is a crucial factor for practical applications, especially considering that LEDs can operate at temperatures up to 150 °C.[46] To evaluate the photostability of the emission at 150 °C, tests were performed for 10 h, both with and without UV illumination (380 nm) on the NaP1-Ag_{66} sample (Figure S17), observing an overall decrease of 4% of the absolute integrated emission. On the other hand, Figure S18 depicts how the integrated emission intensity of the NaP1-Ag_{66} sample slightly decreases as the temperature increases from room temperature to 350 °C. However, upon cooling, a recovery in the intensity is observed, suggesting good reversibility and promising thermal stability. These findings indicate that with further optimization, this single-phase white-light-emitting phosphor could serve as a feasible candidate for an emissive layer in NUV-LED devices.

CONCLUSIONS

In this contribution, the preparation of a Ag-exchanged NaP1 zeolite luminescent material with tunable emission is presented. The successful transformation of a nonconventional precursor, such as natural clinoptilolite, into higher value-added NaP1 zeolite was performed by the hydrothermal method. The as-synthesized NaP1 zeolites were chemically and

https://doi.org/10.1021/acsanm.4c01565
ACS Appl. Nano Mater. 2024, 7, 11965−11972

optically pure to serve as scaffolds to confine and stabilize highly luminescent Ag-NCs, demonstrating that the use of flexible small-pore NaP1 zeolites allows the stabilization of two types of luminescent Ag-NCs with low nuclearity, displaying blue (458 nm) and green-yellow (570 nm) emission bands, tentatively assigned to Ag_3 and Ag_4^{2+} NCs, respectively, generating white light from the combination of both emissive species. The emission color strongly depends on the Ag loadings, where the emission of the samples can be tuned from violet, blue-white, to bright-white, with increasing Ag loadings. Moreover, a pure-white-light emission under NUV excitation (380 nm) with CIE chromaticity coordinates of (0.30, 0.33), an EQE of 6.2%, and excellent thermal stability was achieved for the high-loaded samples. It is expected that these findings could pave the way to novel strategies to obtain cost-effective and small-pore Ag-zeolites from nonconventional precursors and their potential use as sustainable phosphors for white NUV-LED devices.

■ ASSOCIATED CONTENT

Supporting Information

The Supporting Information is available free of charge at https://pubs.acs.org/doi/10.1021/acsanm.4c01565.

Zeolites characterization, used devices, additional SEM-EDS analysis, XPS, DRS, TGA, XRD, steady-state spectra, wide-field fluorescence microscope results, luminescence decay traces, and thermal stability results (PDF)

■ AUTHOR INFORMATION

Corresponding Authors

Eduardo Coutino-Gonzalez − *Sustainable Materials Unit, VITO Flemish Institute for Technological Research, B-2400 Mol, Belgium*; Email: ecoutino@vito.be

Rafael Ramírez-Bon − *Centro de Investigación y de Estudios Avanzados del IPN, Unidad Querétaro, 76001 Querétaro, Querétaro, México*; Email: rrbon@cinvestav.mx

Authors

José Adán Moreno-Torres − *Centro de Investigación y de Estudios Avanzados del IPN, Unidad Querétaro, 76001 Querétaro, Querétaro, México*

Aurore Lecharlier − *E2S UPPA, CNRS, IPREM UMR 5254, Technopôle Hélioparc, Universite de Pau et des Pays de l'Adour, 64053 Cedex 09 Pau, France*

Fabricio Espejel-Ayala − *Centro de Investigación y Desarrollo Tecnológico en Electroquímica, Parque Tecnológico Querétaro, Querétaro 76703, México*

Johan Hofkens − *Molecular Imaging and Photonics, KU Leuven, B-3001 Leuven, Belgium*; orcid.org/0000-0002-9101-0567

Eduard Fron − *Molecular Imaging and Photonics, KU Leuven, B-3001 Leuven, Belgium*; orcid.org/0000-0003-2260-0798

Maarten B. J. Roeffaers − *Centre for Membrane Separations, Adsorption, Catalysis and Spectroscopy for Sustainable Solutions, KU Leuven, B-3001 Leuven, Belgium*; orcid.org/0000-0001-6582-6514

Complete contact information is available at: https://pubs.acs.org/10.1021/acsanm.4c01565

Author Contributions

A.L. prepared the samples and conducted the experiments with the help of J.A.M.-T., F.E.-A., and E.F.; R.R.-B., M.B.J.R., and E.C.-G. conceived and designed the experiments; J.A.M.-T., M.B.J.R., R.R.-B., and E.C.-G. prepared the manuscript with help of all coauthors; all coauthors have given their approval to the final version of the manuscript.

Notes

The authors declare no competing financial interest.

■ ACKNOWLEDGMENTS

E.C.-G. gratefully acknowledges the financial support from CONAHCYT through CB-A1-S-44458 and 2096029-FORDECYT-PRONACES grants. J.A.M.-T. acknowledges the support from a CONAHCYT PhD scholarship (743221).

■ REFERENCES

(1) Pan, L.; Ye, S.; Xv, X.; Lin, P.; Huang, R.; Wang, D. Zeolite-Encaged Luminescent Silver Nanoclusters. *Materials (Basel).* **2023**, *16* (10), 3736.

(2) Haraguchi, N.; Kurosaki, T.; Uchida, S. Small Luminescent Silver Clusters Stabilized in Porous Crystalline Solids. *Phys. Chem. Chem. Phys.* **2024**, *26* (8), 6512−6523.

(3) De Cremer, G.; Coutiño-Gonzalez, E.; Roeffaers, M. B. J.; Moens, B.; Ollevier, J.; Van Der Auweraer, M.; Schoonheydt, R.; Jacobs, P. A.; De Schryver, F. C.; Hofkens, J.; De Vos, D. E.; Sels, B. F.; Vosch, T. Characterization of Fluorescence in Heat-Treated Silver-Exchanged Zeolites. *J. Am. Chem. Soc.* **2009**, *131* (8), 3049−3056.

(4) Fenwick, O.; Coutiño-Gonzalez, E.; Grandjean, D.; Baekelant, W.; Richard, F.; Bonacchi, S.; De Vos, D.; Lievens, P.; Roeffaers, M.; Hofkens, J.; Samorì, P. Tuning the Energetics and Tailoring the Optical Properties of Silver Clusters Confined in Zeolites. *Nat. Mater.* **2016**, *15* (9), 1017−1022.

(5) Grandjean, D.; Coutiño-Gonzalez, E.; Cuong, N. T.; Fron, E.; Baekelant, W.; Aghakhani, S.; Schlexer, P.; D'Acapito, F.; Banerjee, D.; Roeffaers, M. B. J.; Nguyen, M. T.; Hofkens, J.; Lievens, P. Origin of the Bright Photoluminescence of Few-Atom Silver Clusters Confined in LTA Zeolites. *Science (80-.).* **2018**, *361* (6403), 686−690.

(6) Chai, Y.; Shang, W.; Li, W.; Wu, G.; Dai, W.; Guan, N.; Li, L. Noble Metal Particles Confined in Zeolites: Synthesis, Characterization, and Applications. *Adv. Sci.* **2019**, *6* (16), 1900299.

(7) Romolini, G.; Steele, J. A.; Hofkens, J.; Roeffaers, M. B. J.; Coutino-Gonzalez, E. Tunable Luminescence from Stable Silver Nanoclusters Confined in Microporous Zeolites. *Adv. Opt. Mater.* **2021**, *9* (23), 1−13.

(8) Coutino-Gonzalez, E.; Baekelant, W.; Grandjean, D.; Roeffaers, M. B. J.; Fron, E.; Aghakhani, M. S.; Bovet, N.; Van Der Auweraer, M.; Lievens, P.; Vosch, T.; Sels, B.; Hofkens, J. Thermally Activated LTA(Li)-Ag Zeolites with Water-Responsive Photoluminescence Properties. *J. Mater. Chem. C* **2015**, *3* (45), 11857−11867.

(9) Yu, J.; Ye, S.; Liao, H.; Xv, X.; Wang, D. Luminescence Control of Silver Nanoclusters by Tailoring Extra-Framework Cations in FAU-Y Zeolite: Implications for Tunable Emission. *ACS Appl. Nano Mater.* **2021**, *4* (12), 13692−13699.

(10) Lin, H.; Imakita, K.; Fujii, M.; Prokof'ev, V. Y.; Gordina, N. E.; Saïd, B.; Galarneau, A. Visible Emission from Ag^+ Exchanged SOD Zeolites. *Nanoscale* **2015**, *7* (38), 15665−15671.

(11) Li, H.; Yao, D.; Wang, Y.; Li, P. Luminescent Ag^+ Exchanged SOD Zeolites with Their Potential Applications in White LEDs. *Dalt. Trans.* **2020**, *49* (24), 8179−8185.

(12) Tian, X.; Li, Q.; Yao, D.; Li, P.; Li, H.; Wang, Y. Tunable Luminescence of Silver-Exchanged SOD Zeolite Thermally Treated under Mild Conditions. *J. Mater. Chem. C* **2022**, *10* (5), 1666−1671.

(13) Yao, D.; Xu, S.; Wang, Y.; Li, H. White-Emitting Phosphors with High Color-Rendering Index Based on Silver Cluster-Loaded Zeolites and Their Application to near-UV LED-Based White LEDs. *Mater. Chem. Front.* **2019**, *3* (6), 1080−1084.

(14) Baekelant, W.; Romolini, G.; Sun, L.; De Ras, M.; Fron, E.; Moreira, T.; Viola, C.; Ruivo, A.; Laia, C. A. T.; Martens, J.; Martin, C.; Kim, C. W.; Van Der Auweraer, M.; Roeffaers, M. B. J.; Hofkens, J.; Coutino-Gonzalez, E. Tunable White Emission of Silver-Sulfur-Zeolites as Single-Phase LED Phosphors. *Methods Appl. Fluoresc.* **2020**, *8* (2), 024004.
(15) Yao, D.; Yang, J.; Xie, Y.; Wang, Y.; Wang, Y.; Li, H. Warm White-Light Phosphor Based on a Single-Phase of $Ag^{+}/Eu^{3+}/Zn^{2+}$ Loading SOD Zeolites with Application to White LEDs. *J. Alloys Compd.* **2020**, *823*, 153778.
(16) Li, Q.; Tian, X.; Zhao, D.; Wang, Y.; Li, H. Silver Nanoclusters Loaded in Analcime Zeolite for Tunable Luminescence. *ACS Appl. Nano Mater.* **2022**, *5* (9), 13332−13340.
(17) De Waele, V.; Kecht, J.; Tahri, Z.; Mostafavi, M.; Bein, T.; Mintova, S. Diverse Copper Clusters Confined in Microporous Nanocrystals. *Sensors Actuators, B Chem.* **2007**, *126* (1), 338−343.
(18) Goel, S.; Wu, Z.; Zones, S. I.; Iglesia, E. Synthesis and Catalytic Properties of Metal Clusters Encapsulated within Small-Pore (SOD, GIS, ANA) Zeolites. *J. Am. Chem. Soc.* **2012**, *134* (42), 17688−17695.
(19) Aono, H.; Kanayama, K.; Johan, E.; Itagaki, Y.; Matsue, N. Amorphous Materials Prepared by Heat Treatment at Low Temperature for Partially Ag-Exchanged Na-P1 Type Zeolites and Their Photoluminescence Properties. *J. Ceram. Soc. Japan* **2016**, *124* (1), 82−84.
(20) Albert, B. R.; Cheetham, A. K.; Stuart, J. A.; Adams, C. J. Investigations on P Zeolites: Synthesis, Characterisation, and Structure of Highly Crystalline Low-Silica NaP. *Microporous Mesoporous Mater.* **1998**, *21* (1−3), 133−142.
(21) Ghojavand, S.; Dib, E.; Mintova, S. Flexibility in Zeolites: Origin, Limits, and Evaluation. *Chem. Sci.* **2023**, *14* (44), 12430−12446.
(22) Moreno-Torres, J. A.; Espejel-Ayala, F.; Ramírez-Bon, R.; Coutino-Gonzalez, E. Sustainable Strategies to Synthesize Small-Pore NaP Zeolites Using Natural Minerals. *J. Mater. Sci.* **2024**, *59* (2), 423−434.
(23) Ruiz-Serrano, D.; Flores-Acosta, M.; Conde-Barajas, E.; Ramírez-Rosales, D.; Yáñez-Limón, J. M.; Ramírez-Bon, R. Study by XPS of Different Conditioning Processes to Improve the Cation Exchange in Clinoptilolite. *J. Mol. Struct.* **2010**, *980* (1−3), 149−155.
(24) García, G.; Aguilar-Mamani, W.; Carabante, I.; Cabrera, S.; Hedlund, J.; Mouzon, J. Preparation of Zeolite A with Excellent Optical Properties from Clay. *J. Alloys Compd.* **2015**, *619*, 771−777.
(25) Kumon, A.; Abidin, Z.; Matsue, N. Synthesis of Iron Substituted Zeolite with Na-P1 Framework. *J. Porous Mater.* **2017**, *24* (4), 1061−1068.
(26) IZA Copyright © 2017 Structure Commission of the International Zeolite Association. Database of Zeolite Structures. http://www.iza-structure.org/databases/ (accessed 2022-12-20).
(27) Baerlocher, C.; Meier, W. M. The Crystal Structure of Synthetic Zeolite Na-p 1, an Isotype of Gismondine. *Zeitschrift fur Krist. - New Cryst. Struct.* **1972**, *135* (5−6), 339−354.
(28) Huo, Z.; Xu, X.; Lü, Z.; Song, J.; He, M.; Li, Z.; Wang, Q.; Yan, L. Synthesis of Zeolite NaP with Controllable Morphologies. *Microporous Mesoporous Mater.* **2012**, *158*, 137−140.
(29) Zubowa, H. L.; Kosslick, H.; Müller, D.; Richter, M.; Wilde, L.; Fricke, R. Crystallization of Phase-Pure Zeolite NaP from MCM-22-Type Gel Compositions under Microwave Radiation. *Microporous Mesoporous Mater.* **2008**, *109* (1−3), 542−548.
(30) Hildebrando, E. A.; Andrade, C. G. B.; Da Rocha Junior, C. A. F.; Angélica, R. S.; Valenzuela-Diaz, F. R.; De Freitas Neves, R. Synthesis and Characterization of Zeolite NaP Using Kaolin Waste as a Source of Silicon and Aluminum. *Mater. Res.* **2014**, *17*, 174−179.
(31) Bohra, S.; Kundu, D.; Naskar, M. K. Synthesis of Cashew Nut-like Zeolite NaP Powders Using Agro-Waste Material as Silica Source. *Mater. Lett.* **2013**, *106*, 182−185.
(32) Garbowski, E. D.; Mirodatos, C. Investigation of Structural Charge Transfer in Zeolites by Ultraviolet Spectroscopy. *J. Phys. Chem.* **1982**, *86* (1), 97−102.
(33) Rodríguez Iznaga, I.; Petranovskii, V.; Rodríguez Fuentes, G.; Mendoza, C.; Benítez Aguilar, A. Exchange and Reduction of Cu^{2+} Ions in Clinoptilolite. *J. Colloid Interface Sci.* **2007**, *316* (2), 877−886.
(34) Huo, Z.; Xu, X.; Lv, Z.; Song, J.; He, M.; Li, Z.; Wang, Q.; Yan, L.; Li, Y. Thermal Study of NaP Zeolite with Different Morphologies. *J. Therm. Anal. Calorim.* **2013**, *111* (1), 365−369.
(35) Ali, I. O.; El-Sheikh, S. M.; Salama, T. M.; Bakr, M. F.; Fodial, M. H. Controllable Synthesis of NaP Zeolite and Its Application in Calcium Adsorption. *Sci. China Mater.* **2015**, *58* (8), 621−633.
(36) Oleksiak, M. D.; Ghorbanpour, A.; Conato, M. T.; McGrail, B. P.; Grabow, L. C.; Motkuri, R. K.; Rimer, J. D. Synthesis Strategies for Ultrastable Zeolite GIS Polymorphs as Sorbents for Selective Separations. *Chem. - A Eur. J.* **2016**, *22* (45), 16078−16088.
(37) Gui, S. C. R.; Lin, H.; Bao, W.; Wang, W. Effect of Annealing Temperature on Broad Luminescence of Silver-Exchanged Zeolites Y and A. *J. Appl. Spectrosc.* **2018**, *85* (2), 232−238.
(38) Seifert, R.; Rytz, R.; Calzaferri, G. Colors of Ag^{+}-Exchanged Zeolite A. *J. Phys. Chem. A* **2000**, *104* (32), 7473−7483.
(39) Aghakhani, S.; Grandjean, D.; Baekelant, W.; Coutiño-Gonzalez, E.; Fron, E.; Kvashnina, K.; Roeffaers, M. B. J.; Hofkens, J.; Sels, B. F.; Lievens, P. Atomic Scale Reversible Opto-Structural Switching of Few Atom Luminescent Silver Clusters Confined in LTA Zeolites. *Nanoscale* **2018**, *10* (24), 11467−11476.
(40) Wang, Y.; Herron, N. Photoluminescence and Relaxation Dynamics of CdS Superclusters in Zeolites. *J. Phys. Chem.* **1988**, *92* (17), 4988−4994.
(41) Fron, E.; Aghakhani, S.; Baekelant, W.; Grandjean, D.; Coutino-Gonzalez, E.; Van Der Auweraer, M.; Roeffaers, M. B. J.; Lievens, P.; Hofkens, J. Structural and Photophysical Characterization of Ag Clusters in LTA Zeolites. *J. Phys. Chem. C* **2019**, *123* (16), 10630−10638.
(42) Coutino-Gonzalez, E.; Roeffaers, M. B. J.; Dieu, B.; De Cremer, G.; Leyre, S.; Hanselaer, P.; Fyen, W.; Sels, B.; Hofkens, J. Determination and Optimization of the Luminescence External Quantum Efficiency of Silver-Clusters Zeolite Composites. *J. Phys. Chem. C* **2013**, *117* (14), 6998−7004.
(43) Plessers, E.; van den Reijen, J. E.; de Jongh, P. E.; de Jong, K. P.; Roeffaers, M. B. J. Origin and Abatement of Heterogeneity at the Support Granule Scale of Silver on Silica Catalysts. *ChemCatChem* **2017**, *9* (24), 4562−4569.
(44) Fleury, G.; Roeffaers, M. B. J. Correlating Acid Site Distribution and Catalytic Activity in Dealuminated Mordenite at the Single-Particle Level. *ACS Catal.* **2020**, *10* (24), 14801−14809.
(45) Choi, H. J.; Min, J. G.; Ahn, S. H.; Shin, J.; Hong, S. B.; Radhakrishnan, S.; Chandran, C. V.; Bell, R. G.; Breynaert, E.; Kirschhock, C. E. A. Framework Flexibility-Driven CO_2 Adsorption on a Zeolite. *Mater. Horizons* **2020**, *7* (6), 1528−1532.
(46) Zhou, X.; Feng, X.; Yin, J.; Zhang, X.; Li, P.; Li, H. High-Quantum-Efficiency Blue Phosphors with Superior Thermal Stability Derived from Eu^{3+}-Doped Faujasite Y Zeolite. *Inorg. Chem.* **2023**, *62* (42), 17547−17554.

https://doi.org/10.1021/acsanm.4c01565
ACS Appl. Nano Mater. 2024, 7, 11965−11972